EFFECTS OF RARE EARTH OXIDES ON SOME PHYSICAL PROPERTIES OF LI- ZN NANOPARTICLE FERRITES

M. A. AHMED [1], N. OKASHA[2], A. I. ALI [3]*, M. HAMMAM[3] and J. Y. SONG[4]

[1] *Materials Science Lab (1), Physics Department, Faculty of Science, Cairo University, Giza, Egypt*
[2] *Physics Department, Faculty of Girls, Ain Shams University, Cairo, Egypt*
[3] *Physics Department, Helwan University Ain Helwan, 11795, Cairo, Egypt.*
[4] *Department of Materials Science and Engineering, Pohang University of Science and Technology (POSTECH), Pohang 790-784, Korea.*

Abstract

The spinel ferrite $Li_{0.2}Zn_{0.6}La_yFe_{2.2-y}O_4$; $0.01 \leq y \leq 0.1$ were prepared by the usual ceramic sintering technique. XRD confirmed the formation of the samples in single phase spinel structure for all the samples. The lattice parameters decreased with increasing the La-content. The d c resistivity was measured as a function of temperature. The obtained results indicate the semiconductor like behavior, where more than straight lines indicating the presence of different conductions mechanism exist. The density of states near Fremi level as a function of La-content and discussed based on the variable range hoping model. The dielectric constant and dielectric loss were measured as a function of temperature and frequency. The dispersion peak at low frequency (10 kHz) was splitted by increasing La-content up to the suggested absorber splitting.

1. Introduction

Li-Zn-Ferrites have high potential for several electromagnetic devices in the radio frequency region, since they have frequency-dependent physical properties, such as permittivity and permeability. Polycrystalline ferrite has been extensively used in many electronic devices because of its high permeability in the radio frequency region, high electrical resistivity, mechanical toughness and chemical stability. There are many experimental and theoretical investigations on the frequency dispersion of complex permeability in polycrystalline ferrite [1- 6]. The complex permeability spectra of polycrystalline ferrite depend not only on the chemical composition of the ferrite but also on the post-sintering density and the microstructure such as grain size and porosity. These are attributed to the fact that the permeability of the polycrystalline ferrite is described as the superposition of two different magnetizing processes: spin rotation and

domain wall motion [1, 6 and 7]. It is known that there are much applications of polycrystalline ferrite in the radio frequency devices. Lithium based ferrite is a pertinent magnetic material for applications because of its better properties of high frequency (high resistivity), high Curie temperature, low dielectric loss and lower densification temperature than NiZn ferrite. It is known that the preparation of Liz ferrite in dense polycrystalline form by conventional ceramic processing is difficult because of the Lithia evaporation implies a limitation of the sintering temperature.

Some authors [8-10] have been reported on the effect of the addition of divalent, trivalent and tetravalent ions on the electrical conductivity and dielectric properties. The electrical properties of mixed Li- Cd ferrites were reported by Ravinder and Radha [12] have studied the Li- Cd ferrites for their frequency

and composition dependence of dielectric behavior.

Some researches have studied the influence of La-content on ferromagnetic oxides [15- 19]. D. Ravider et al [18, 19] studied the influence of the rare earth atoms with a large radius and stable valance (3^+) such as Gd_2O_3 and La_2O_3 in modification the ferrites structure and properties, where they measured at low frequency (1kHz or 1MHz). Moreover, they could not explain the effect of different amounts of rare earth on the dielectric properties.

In the present work, we aimed to study the effect of La substitution on the structure and the transport properties of the $Li_{0.2}Zn_{0.6}La_yFe_{2.2-y}O_4$; $(0.01 \leq y \leq 0.1)$ system in the high temperature region as a function of frequency and temperature. Also one of our goals was to reach the critical concentration at which the physical properties reach the optimum values and the sample become more applicable.

2. Experimental procedures
a- Sample preparation:

High purity oxides of Fe_2O_3, LiOH, ZnO and La_2O_3 were mixed together in molar ratio to prepare ferrites of composition $Li_{0.2}Zn_{0.6}La_yFe_{2.2-y}O_4$ $(0.01 \leq y \leq 0.1)$ using the conventional double sintering technique. Final sintering of the specimens was carried out for 15h at 1150°C. The details of the method of preparation have been given in our earlier publication [20].

b- Characterization and measurements:

X- ray powder diffraction was performed on the investigated samples using Rigaku Co- Miniflex X- ray diffractometer employing CuK radiation with λ=1.5418Å.The particle size (D) was calculated

using Scherer's relationship, $D = 0.9\lambda /\beta\cos\theta$; where λ is the X- ray wavelength, θ is the Bragg's diffraction angle and β is the half width of the (311) XRD peaks. The complex dielectric properties measurements were carried out using programmable automatic LCR-Meter (HP model 4284A) in the frequency range of 100 Hz ~ 1 MHz. The dielectric constants were measured for both heating and cooling runs. The cooling rate was about 0.6 K/min, and the sample temperature was monitored with a copper-constantan thermocouple connected to a Keithley 2000 digital multimeter. Electrical resistivity was measured both on cooling and heating runs in the temperature range from 10 K to 300 K by standard dc four-probe method using a CCR type refrigerator in NIT (Nanotechnology and Information Lab., Pusan National University, Busan, Korea).

3. Results and discussion
3. a. The structural analysis:

XRD diffraction pattern of the $Li_{0.2}Zn_{0.6}La_yFe_{2.2-y}O_4$ $(0.01 \leq y \leq 0.1)$ system
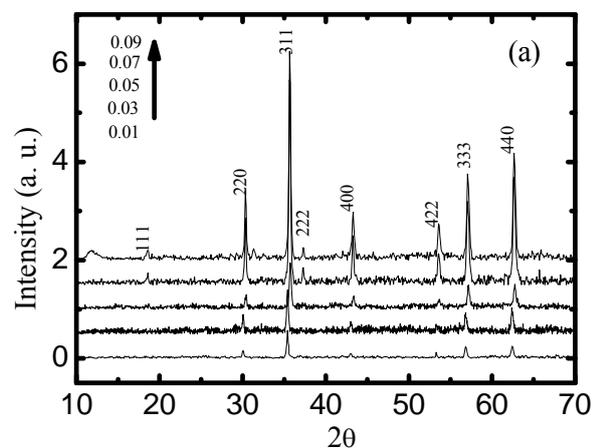

Fig. (1): a- XRD patterns for $Li_{0.2}Zn_{0.6}La_yFe_{2.2-y}O_4$ system.

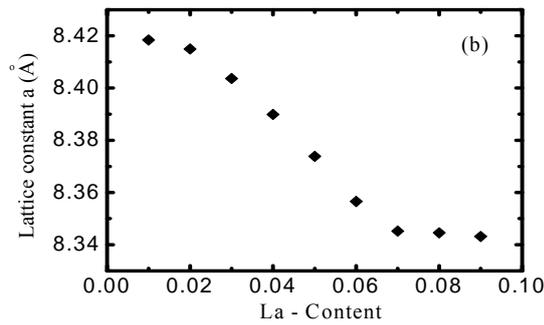was shown in Fig. (1a).

The spectra indicate that, there is

Fig. (!): b- The change of lattice constant (a) with La content**.**

nanocrystalline ferrites with no extra reflections and cubic structure belong to fcc spinel structure crystal symmetry was obtained. This result was good agreement with the previous studies on Li-Zn ferrite [12, 13, 17]. The lattice constant, (a) is plotted as a function of y in Fig. (1b) where the values of (a) is agree well with JCPDS card [21], within experimental errors. It is clear that, the value of (a) decreases with increasing La-content up to y=0.07 then reach stable values. This behavior can be explained as follows: due to increase of the heat treatment, the magnetic domains will be increased leading to an increase in the crystallite size for all samples. When some Fe^{3+} ions in ferrite lattice were substituted by La ions, the lattice constant will be changed [22, 23]. The variation of lattice constant leads to an increase in the lattice strains which produce an internal stress [24, 25]. Such a stress hinders the growth of grains, so the particle sizes of the samples doped with La ions are smaller than that of Li- Zn ferrite nanoparticle. On the other hand, due to the

larger bond of La^{3+}- O^{2-} as compared with that of Fe^{3+}- O^{2-}, it is obvious that more energy is needed to make La ions enter into lattice and form La^{3+}- O^{2-} bonds. All doped La^{3+} ferrite have higher thermal stability relative to Li- Zn ferrite nanocrystalline, and hence more energy is needed for the substituted samples to complete the crystallization and grow grains.
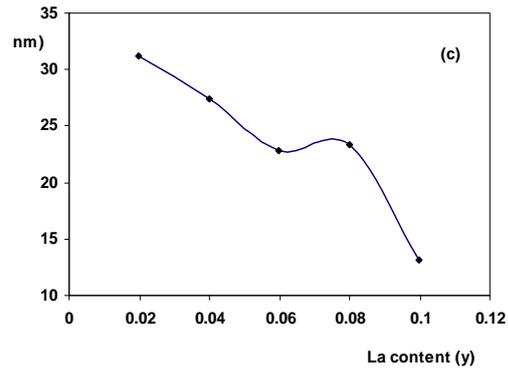

Fig. (1): c- The change of particle size (D) with La content.

reside on the grain boundary as the ionic radii of La^{3+} ions is larger than that of Fe^{3+} ions. The average particle size (D) was calculated and shows in Fig. (1c).

It is reasonable to observe that, the particle sizes (D) for all concentrations were decreased with increasing La content where the presence of La ions on the grain boundary, cause pressure on the grains leads to hinder the growth of the grains as mentioned before.

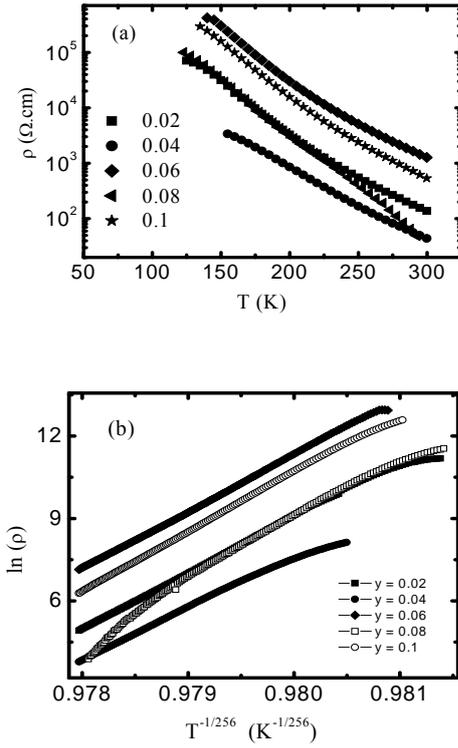*3-b. The electrical properties:*

Fig. (2): a- The electrical resistivity as a function of temperature, b- The logarithms of the electrical conductivity Vs. $1/T^{1/256}$ for the investigated samples.

The electrical resistivity as a function of temperature has been summarized in Fig. (2a). The resistivity of all compositions show insulating behavior, which gives an increasing resistance with decreasing temperature, from room temperature down to 100 K. To know the type of conduction mechanism, we checked the resistivity variation as a function of temperature, 1000/T, and the hopping mechanism $(1/T)^{1/2}$.

The temperature dependent on resistivity for all compositions can be well described by the variable range hopping (VRH) model [14],

depicted in Fig. (2b). In the VRH model, the resistivity of compositions is given by,

$$\rho = \rho_o \exp(\frac{T_o}{T})^{\frac{1}{4}} \tag{1}$$

where To is the reduced temperature which is related to the localization length by,

$$T_o = \beta / k_B g(\mu) a_o^3 \tag{2}$$

where β is the numerical factor, k_B is the Boltzmann's constant, $g(\mu)$ is the electronic density of states, and a_o is the Bohr radius[15]. From the plot of ln (ρ) versus $T^{1/256}$, we have estimated the fitting factor (To) as shown with La-content in Fig. (2b), to acceptable values which are around 6×10^9 K.

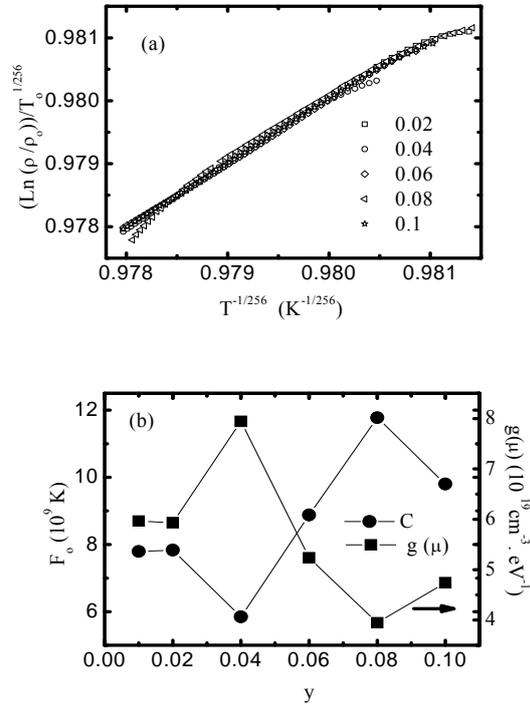The density of state g (m) versus La concentration (y) is shown in Fig. (3b).

Fig. (3): a- The master plot of the reduced electrical resistivity Vs reduced temperature,
b- Density of state g (m) and fitting temperature as a

4

The data shows that for the low doping compositions (y = 0.01 and 0.02) the density of state has nearly constant values $5 \sim 6 \times 10^{19}$ cm^{-3}.eV^{-1}. However, it increased with an increasing in y from 0.03 to 0.04 to become 12×10^{19} cm^{-3}.eV^{-1}). It was decreased down to minimum values with the highest doping composition (y = 0.1).

To confirm the fitting for all compositions, we draw the master plot for ((ln (ρ) + Ln (ρo))/(To) $^{1/4}$) Vs T$^{-1/4}$ as shown in Fig. (3a) providing an excellent fit to eq. (1) [14–17]. We can conclude that, since La^{3+} contents can change the Fe^{2+}/Fe^{3+} ratio, it is reasonable to assume that g(m) is nearly dependent on La-content. Therefore, the variation of to and g (m) with La-content reflects the change of localization length. This implies that the disorder in the lattice decreases with La-doping. As the extent of disorder decreases with La-doping, it is evident from Fig.(2) and Fig. (3), that the conduction mechanisms in this material are not thermally activated but are related to the hopping between Fe^{2+} and Fe^{3+} ions.

3-c: The dielectric properties:

Figure (4:a-d) shows the dependence of the dielectric constant (έ) on the absolute temperature for Li$_{0.2}$Zn$_{0.6}$La$_y$Fe$_{2.2-y}$O$_4$ system at different frequencies 10kHz, 100kHz, and 1MHz.
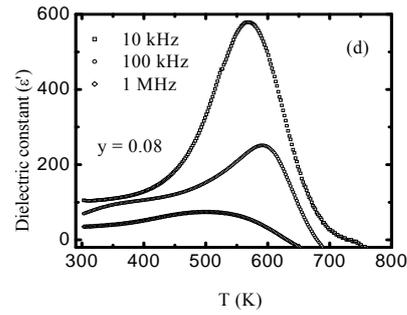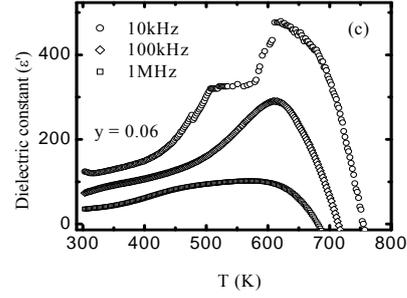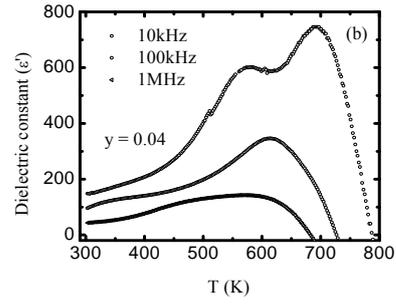

Fig.(4:a-d): The dielectric constant as function of temperature for Li$_{0.2}$Zn$_{0.6}$La$_y$Fe$_{2.2-y}$O$_4$ system at different frequencies 10kHz, 100kHz, and 1MHz with La-contents.
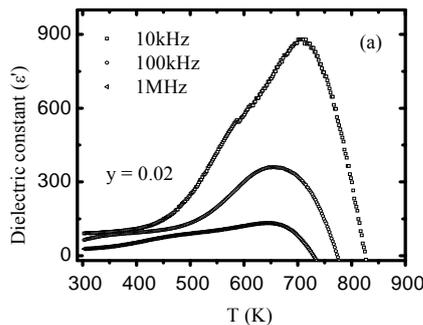
We presented here two samples depending on the La-contents at y = 0.02, 0.04. From the obtained data it is clear that the dielectric constant is kept constant from 300 K up to 450 K. With increasing the temperature around 500 K, the dielectric constant start to increase and a sharp peak appeared around 700 K at the applied frequency 10 kHz, while this peak is shifted to lower temperature (650 K) at frequency 100 kHz and decreased to the lowest temperature (625 K) when the applied

frequency become 1MHz. This means that, at low temperature region (T < 450 K), the dipoles were frozen as well as the polarization is low, as a result, the dielectric constant gives no observable change in έ. With an increasing the temperature up to 500 K, the dipoles starts to thermally activated as a results of increasing the polarization and the dielectric constant increases. Further increasing temperature up to 700 K the thermal energy increases the lattice vibrations and the polarization as well as έ was to reach the smaller values.

One of the most important features here is that with applying the low electric field at (10 kHz) as in Fig. (5: a- c),
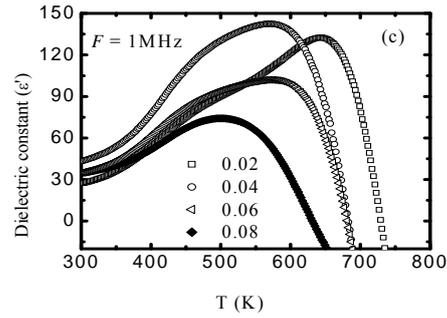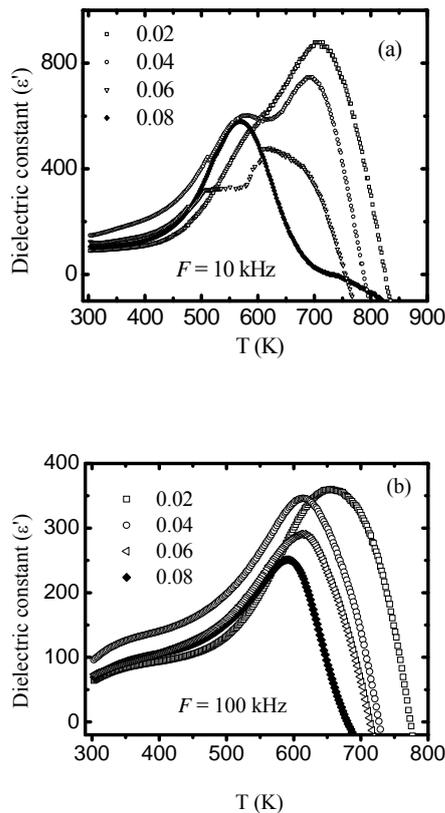
Fig.(5:a- c): The dielectric constant as function of temperature with different La-contents and at different frequencies (a) 10 kHz (b) 100 kHz. and (c).

The dielectric constant gives the highest value while its value decreases with increasing the frequency. This can be explained as due to applying the low frequency the dipole moments rotates very fast and can not fallow the field variation with the result of the decreasing έ with increasing the frequency. At low frequency more dipoles become free and the field aligned them in its direction leading to an increase in polarization and έ. Moreover, the data in the Figure pronounced that the plateau region of (ε') extends up to T = 400 K. This relaxation is supposed to be arising from the electron hopping mechanism between the iron ions of different valances as reported for other ferrites containing Fe^{2+} ions [26- 28].

Therefore, Fe^{3+} produced from Fe^{2+} ion initiate vacancies which would form pairs with Fe^{2+} ions and give rise to electron hopping analogous to the general behavior of ferrites. Accordingly, the values of dielectric constant increase with increasing temperature for all La concentrations. This behavior of (ε') with temperature for the investigated samples agrees well with the known spinel ferrites [29] where (ε') increases with increasing temperature and decreases with increasing frequency. The

increase of (ε') with temperature in this group can be ascribed to the cooperation of more than one type of polarization from room temperature up to 650 K. The electronic polarization is the most predominant one under the effect of both small thermal energy and applied electric field. With increasing frequency, the scattering processes between s–s and s–d interbands take place due to electron phonon interaction which decreases the intergranular spacing giving rise the same hopping length in both tetrahedral and octahedral sites. Rabkin et al. [30] suggested that, the processes of dielectric polarization in ferrites take place through a mechanism which is the same as that of conduction process because of the two processes are of the same origin. Due to electronic exchange $Fe^{2+} \rightarrow Fe^{3+} + e^-$, one can obtain local displacements of charge in the direction of the applied electric field, these displacements determine the polarization. Both types of charge carriers n and p contribute to polarization and they depend on temperature. Since the influence of temperature on the electronic exchange $Fe^{2+} \rightarrow Fe^{3+}$ is more pronounced than on the displacement of P-carriers, ε' will be increased rapidly with increasing temperature. Indeed, this behavior can be seen clearly for various La concentrations.

4. Conclusions

XRD patterns show that, the investigated ferrite has single spinel structure. The lattice constant are decreased with increasing La content up to 0.07 then stable where all doped La ions cannot enter into the lattice but reside on the grain boundary and this lead to decrease in the particle size. The decrease in dielectric constant with increasing frequency for all samples is attributed to the decrease in the

polarization because of the dipoles cannot follow up the field variation. The dielectric losses are reflected on the conductivity measurements where the materials of high conductivity exhibiting high losses and vice versa. Finally, this study was an attempt to improve the quality of the classic Li- Zn ferrite by introducing different substitution of R_2O_3 instead of Fe_2O_3.

References

1. G.T. Rado Rev. Mod. Phys. 25 (1953) 81.

2. D. Polder and J. Smit Rev. Mod. Phys. 25 (1953) 81.

3. J. Smit and H.M.J. Wijn Ferrites, Phillips Technical Library, Eindhoven, the Netherlands (1959).

4. E. Scloemann J. Appl. Phys. 41 (1970) 204.

5. A. Globus J. Phys. C 1 (1977) 1.

6. J.P. Bouchaud and P.G. Zerah J. Appl. Phys. 67 (1990) 5512.

7. Y. Naito, Proceedings of the First International Conference on Ferrites, (1970) 558.

8. S. A. Mazen, Phys. Stat. Sol. (a) 154 (1996)681.

9. A. Ahmed, J. Mater. Sci., 27 (1992)4120.

10. S. A. Mazen, F. Metawe, S. F. Mansour, J. Phys. D: Appl. Phys., 30 (1997)1799.

11. D. Ravinder, T. S. Res, Crys. Res. Technol., (Est Germany) 25 (8) (1990)963.

12. K. Radha, D. Ravinder, Indian J. Pure & Appl. Phys., 33 (1995)74.

13. Yang Ying- Chang, Kong Lin- Shu, Sun Shu- he, Gu Dong- mei, J. Appl. Phys., 63 (1988)3702.

14. Li Hong- Shuo, Hu Bo- Ping, Coey J. M. D., Solid State Commun., 66 (1988)133.

15. N. Rezlescu, E. Rezlescu, C. Pasnicu, M. L. Craus, J. Phys., 6 (1994)5707.

16. N. Rezlescu, E. Rezlescu, C. Pasnicu, M. L. Craus, J. Mag. Mag. Mater., 136 (1994)319.

17. N. Rezlescu, E. Rezlescu, P. D. Popa,, L. Rezlescu, J. Alloys Compounds, 275 (1998)657.

18. D. Ravinder, B. Ravi Kumar, J. Materials letters 57 (2003)1738.

19. T. Nakamura, K. Hatakeyama IEEE Trans. Magn., 365 (2000)3415.

20. M.A.Ahmed, N. Ocasha, and A. I. Ali, J. Applied Physics D, 2007 (under publication).

21. JCPDS- ICDD (c) (1991).

22. N. Rezlescu, E. Rezlescu, C. Pasnicu, M. L. Craus, J. Mag. Mag. Mater., 136 (1994)319.

23. A. A. Satar, A. M. Samy, R. S. El-Ezza, A. E. Eatah, Phys. Stat. Solidi, A. Appl. Res., 193 (1) (2002)86.

24. Hua Yang, Zichen Wang, Lizhu Aong, Muyu Zhao, Jianping Wang, Heli Luo., J. Phys. D. Appl. Phys., 29 (1996)2574.

25. Hua Yang, Lijun Zhao, Xuwei Yang, Lianchun Shen, Lianxiang Yu, Wei Sun, Yu Yan, Wenquan Wang, Shouhua Feng, J. Mag. Mag. Mater., 271 (2004)230.

26. 26 S.T. Mahmuda, A.K.M. Hossaina, A.K.M. Abdul Hakimb, M. Sekic,T. Kawaic, H. Tabata, Journal of Magnetism and Magnetic Materials 305 269–274 (2006).

27 S.A. Morrison, C.L. Cahill, R. Swaminathan, M.E. McHenry, V.G. Harris, J. Appl. Phys. 95 (11) 6392 (2004).

28. T. Nakamura, M. Naoe, Y. Yamad, Journal of Magnetism and Magnetic Materials (305)120–126 (2006).

29. S. F. Mansour, Egypt. J. Solids, Vol. (28), No. (2), (2005).

30. D. Ravinder , A.V. Ramana Reddy, Materials Letters (38) 265–269 (1999).